Thyroid hormone receptor α in skeletal muscle is essential for T3-mediated increase in energy expenditure

Trine S Nicolaisen, Anders B Klein, Oksana Dmytriyeva, Jens Lund, Lars R Ingerslev, Andreas M Fritzen, Christian S Carl, Anne-Marie Lundsgaard, Mikkel Frost, Tao Ma, et al.

Thyroid hormone receptor α in skeletal muscle is essential for T3-mediated increase in energy expenditure

Trine S. Nicolaisen[1,2*], Anders B. Klein[1*], Oksana Dmytriyeva[1, 3], Jens Lund[1], Lars Ingerslev[1], Andreas M. Fritzen[2], Christian S. Carl[2], Anne-Marie Lundsgaard[2], Mikkel Frost[1], Tao Ma[1], Peter Schjerling[4], Zachary Gerhart-Hines[1], Frederic Flamant[5], Karine Gauthier[5], Steen Larsen[6], Erik A Richter[2], Bente Kiens[2] and Christoffer Clemmensen[1#]

[1]Novo Nordisk Foundation Center for Basic Metabolic Research, Faculty of Health and Medical Sciences, University of Copenhagen, Copenhagen, Denmark
[2]Section of Molecular Physiology, Department of Nutrition, Exercise and Sports, Faculty of Science, University of Copenhagen, Copenhagen, Denmark
[3]Department for Biomedical Research, Faculty of Health Sciences, University of Copenhagen, Denmark
[4]Institute of Sports Medicine Copenhagen, Department of Orthopedic Surgery, Bispebjerg-Frederiksberg Hospital and Center for Healthy Aging, Faculty of Health Sciences, University of Copenhagen, Denmark
[5]Institut de Génomique Fonctionnelle de Lyon, INRA USC 1370, Université de Lyon, Université Lyon 1, CNRS UMR 5242, Ecole Normale Supérieure de Lyon, Lyon, France
[6]Xlab, Center for Healthy Aging, Department of Biomedical Sciences, Faculty of Health and Medical Sciences, University of Copenhagen, Copenhagen, Denmark

[*]Co-first author

Correspondence: Christoffer Clemmensen, chc@sund.ku.dk

HIGHLIGHTS

- Thyroid hormone receptor alpha 1 (TRα_1) is critical for fiber type composition in slow twitch muscle.
- TRα_1 loss-of-function in skeletal muscle does not affect exercise capacity or voluntary running.
- In the absence of muscle TRα_1, increased sarcolipin expression might safeguard basal metabolic rate and exercise capacity.
- Thyroid hormone-induced increase in metabolic rate (thyroid thermogenesis) is dependent on TRα_1 in skeletal muscle.
- Thyroid hormone-induced elevation in body temperature is independent of skeletal muscle TRα_1.

ABSTRACT

Thyroid hormones are important for homeostatic control of energy metabolism and body temperature. Although skeletal muscle is considered an important site for thyroid action, the contribution of thyroid hormone receptor signaling in muscle to whole-body energy metabolism and body temperature has not been resolved. Here, we show that thyroid hormone (T3)-induced increase in energy expenditure requires thyroid hormone receptor alpha 1 ($TR\alpha_1$) in skeletal muscle, but T3-mediated elevation in body temperature is independent of muscle-$TR\alpha_1$. In slow-twitch soleus muscle, loss-of-function of $TR\alpha_1$ ($TR\alpha^{HSACre}$) alters fiber type composition toward a more oxidative phenotype. The change in fiber type composition, however, does not influence running capacity or motivation to run. RNA-sequencing of soleus muscle from WT mice and $TR\alpha^{HSACre}$ mice revealed differentiated transcriptional regulation of genes associated with muscle thermogenesis, such as sarcolipin and UCP3, providing molecular clues pertaining to the mechanistic underpinnings of $TR\alpha_1$-linked control of whole-body metabolic rate. Together, this work establishes a fundamental role for skeletal muscle in T3-stimulated increase in whole-body energy expenditure.

INTRODUCTION

Thyroid hormones (triiodothyronine (T3) and thyroxine (T4)) influence a multitude of physiological functions mirrored by the ubiquitous expression of thyroid hormone receptors throughout the body (Mullur et al., 2014). Notably, excess thyroid hormone production (hyperthyroidism) or administration of exogenous thyroid hormone potently increases energy metabolism (Mullur et al., 2014). Cumulative evidence underscores that this endocrine effect, oftentimes referred to as 'thyroid thermogenesis,' involves both central and peripheral mechanisms of action (Mullur et al., 2014). In context, thyroid hormone-induced stimulation of muscle and liver Na^+/K^+ ATPase activity, as well as induction of futile cycling of Ca^{2+} between cytoplasm and sarcoplasmic reticulum in muscle, has undergone considerable scientific scrutiny (Silva, 2006). Sympathetic nervous system (SNS)-induced brown adipose tissue (BAT) non-shivering thermogenesis also has been linked to thyroid thermogenesis (Silva, 2006). Activation of the SNS induces expression of the enzyme deiodinase type 2 (DIO2), which facilitates the conversion of T4 to T3 that, in turn, increases expression of uncoupling protein 1 (UCP1) in BAT (Silva and Larsen, 1983, 1985). Further, central T3 actions activate BAT thermogenesis via an AMP-activated kinase (AMPK)-dependent mechanism in the hypothalamus, emphasizing the importance of BAT as a primary site for thyroid thermogenesis (Lopez et al., 2010).

Surprisingly, two independent investigations recently reported that BAT thermogenesis is dispensable for thyroid hormone-induced increase in energy expenditure (Dittner et al., 2019; Johann et al., 2019). It was reported that although thyroid hormones substantially increase UCP1 in BAT and induce browning of inguinal white adipose tissue (iWAT), these changes do not translate to an increased metabolic rate. In fact, thyroid hormone-induced increases in energy expenditure, body temperature, and food intake were similar between UCP1 knock-out (KO) and wild-type (WT) mice (Dittner et al., 2019). While Dittner and colleagues (2019) speculated that thyroid thermogenesis might be secondary to thyroid hormone-induced elevation in body temperature governed by the brain, Johann et al., (2019) hypothesized that stimulation of the thyroid hormone receptor alpha 1 ($TR\alpha_1$) in slow-twitch muscle contributes to T3-associated hyperthermia.

To resolve whether thyroid hormone action in skeletal muscle is necessary for thyroid thermogenesis and the associated increase in body temperature, we developed a skeletal muscle-specific $TR\alpha_1$-dominant negative mouse model ($TR\alpha_1$ loss-of-function). Notably, we discovered that under normal and metabolically compromised conditions, the T3-mediated increase in whole-body energy expenditure, in part, relies on thyroid actions via $TR\alpha_1$ signaling in muscle, but T3-induced hyperthermia is independent of $TR\alpha_1$ signaling in muscle.

RESULTS

Skeletal muscle TRα$_1$ defines fiber type composition in slow-twitch muscle but is largely dispensable for exercise capacity and energy homeostasis

To study the role of thyroid hormone receptor signaling in skeletal muscle on whole-body energy metabolism, we generated a skeletal muscle-specific TRα$_1$ loss-of-function mouse model (TRα^{HSACre}) (Fig. S1A-C). Because this mouse model has not been characterized previously, we initially sought to determine the impact of skeletal muscle TRα$_1$ mutation on whole-body energy metabolism under normal physiological conditions and in the context of exercise stress and high-fat diet (HFD)-induced obesity. Plasma concentrations of T3 and T4 were similar between chow-fed TRα^{HSACre} and WT littermate controls (Fig. 1B-C). No differences in body weight, fat and lean mass, or glucose tolerance were observed between genotypes (Fig. 1D-F). Exhaustive running capacity on treadmill and voluntary wheel running, measured for 6 weeks, also were not different between genotypes (Fig. 1G-H).

Another cohort of animals was fed a HFD for 22 weeks and had a slower weight gain trajectory for the TRα^{HSACre} mice relative to the WT mice in response to the dietary challenge (Fig. 1J), which could not be explained by differences in food intake (Fig. 1K). Following 18 weeks of HFD exposure, the TRα^{HSACre} mice weighed the same as the WT mice. No genotype differences in body composition, glucose tolerance, or body temperature in response to a moderate cold challenge (14° for 4 h) were found in the weight-matched HFD fed mice (Fig. 1L-N). Notably, TRα^{HSACre} mice displayed an increase in type I fibers and a decrease in type IIA fibers in slow-twitch soleus muscle (SOL) compared to WT mice (Fig. 1P). This difference, however, was not present in fast-twitch extensor digitorum longus (EDL) muscle (Fig. 1Q). The fiber-type switch in slow-twitch muscle was accompanied by an increase (72%) in circulating growth differentiation factor 15 (GDF15), a systemic marker of cellular and mitochondrial stress (Fig. 1R). In summary, TRα$_1$ is required for establishing and/or maintaining slow-twitch muscle fiber-type composition, yet mutation of TRα$_1$ function in muscle has no major consequences for energy metabolism, glucose tolerance, or exercise capacity.

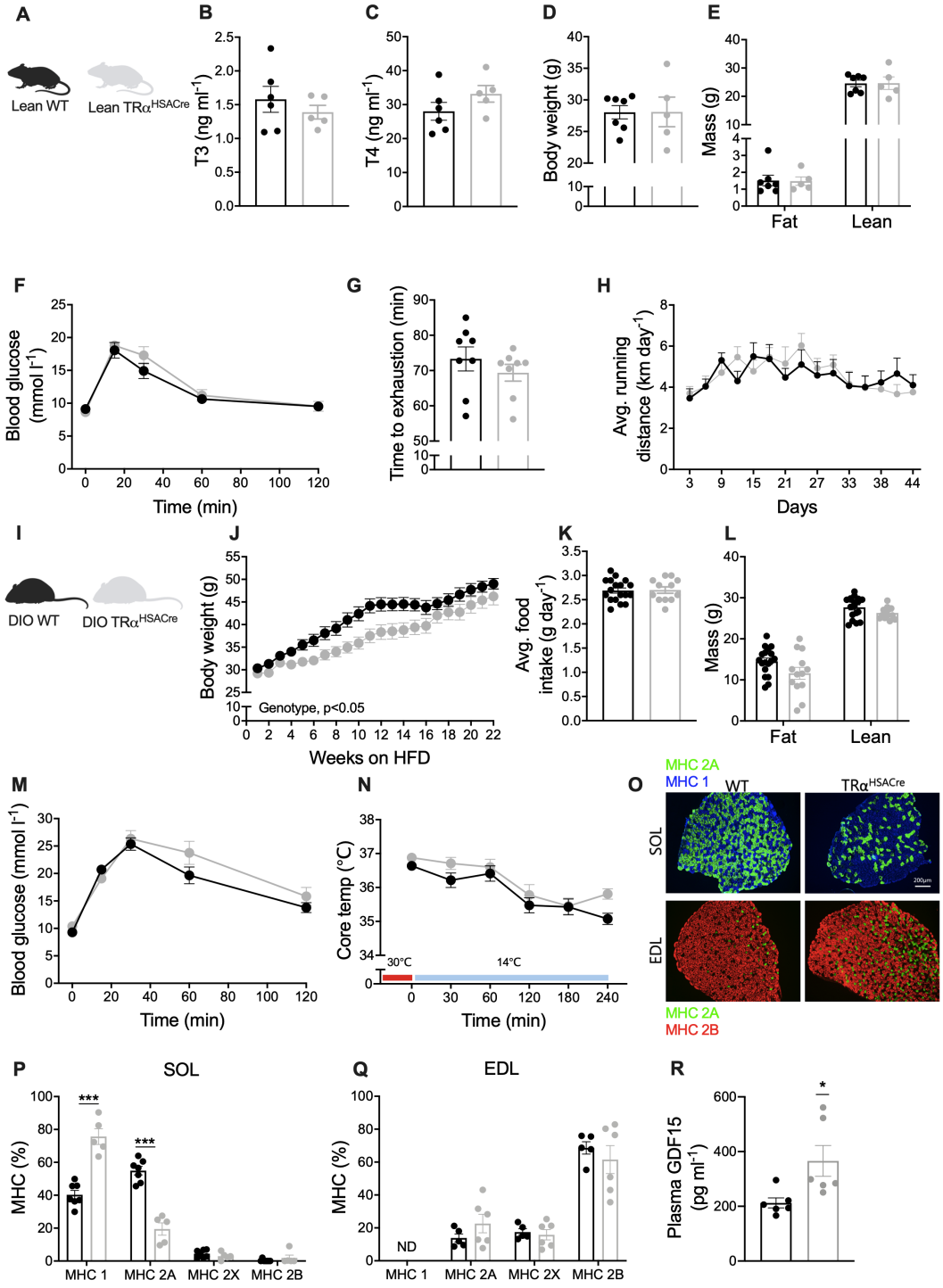

Figure 1. Skeletal muscle TRα$_1$ is crucial for muscle morphology but plays a minor role in energy and glucose metabolism.

A, Wild-type (WT) (black) and TRα^{HSACre} (gray) mice were characterized on a chow diet. **B**, Plasma T3 (**C**) and T4 concentrations, (**D**) body weight, (**E**) body composition, (**F**) glucose tolerance, (**G**) exercise capacity on a treadmill, and (**H**) average daily running distance during 44 days of voluntary wheel running (lean WT/TRα^{HSACre}, n=7-8/5-10). **I**, Another cohort of mice were exposed to diet-induced obesity (DIO), WT (black) and TRα^{HSACre} (gray). **J**, Effects on body weight, (**K**) food intake, (**L**) body composition, (**M**)

glucose tolerance (DIO WT/TRα^{HSACre}, n=18/12-13). **N**, Core temperature at thermoneutrality and during a mild cold challenge (DIO WT/TRα^{HSACre}, n=8/10). **O**, **P**, **Q**, Fiber type distribution in SOL and EDL muscles and (**R**) circulating GDF15 levels (DIO WT/TRα^{HSACre}, n=5-7/5-6). Unpaired t-test in **B-E**, **G**, **K**, **L,** and **P-R** was applied to test for genotype differences, and a two-way ANOVA with a Bonferroni post hoc test in **F**, **H**, **J**, **M,** and **N**, was applied to evaluate effects of genotype and time. Post hoc analyses were performed irrespective of ANOVA results. *** $p < 0.001$, * $p < 0.05$. All data are presented as mean ± SEM.

TRα$_1$ in skeletal muscle is required for T3-induced energy expenditure but is dispensable for T3-induced elevation in body temperature

To study the importance of skeletal muscle TRα$_1$ on thyroid hormone-induced energy expenditure, TRα^{HSACre} and WT littermates were treated daily for five days with subcutaneous injections of T3, resulting in increased T3 but decreased T4 plasma concentrations (Fig. S1D-G). Indirect calorimetry revealed an increase in energy expenditure in response to T3 treatment in lean WT mice (20% increase in the light cycle and 24% increase in the dark cycle, respectively). Conversely, T3 treatment did not significantly increase energy expenditure in lean TRα^{HSACre} mice (Fig. 2B-C). In DIO WT mice the effect of T3 on metabolic rate was more pronounced that in the lean WT mice suggesting that the thermogenic effect of T3 is related to fat mass. In this context, it may be that the absence of functional TRα$_1$ in muscle will have less impact on energy expenditure in DIO mice, than in a lean mouse. Accordingly, during the day T3-mediated increase in metabolic rate was similar in WT and TRα^{HSACre} mice, whereas during dark cycle, T3-induced energy expenditure was only found in WT mice. The consecutive increase in T3-mediated increase in energy expenditure in DIO mice is similar to what we have previously observed in this dietary model (Finan et al., 2016).

To decipher the muscle-specific effect of T3 on mitochondrial respiration in chow-fed WT and TRα^{HSACre} mice, slow-twitch (SOL) and fast-twitch (EDL) muscles were excised from T3-treated mice and assessed for mitochondrial respiratory capacity (Fig. 2G-H). In SOL muscle, leak respiration (state 2) was similar between genotypes, but, in the context of T3 treatment, respiration only increased in WT mice, mirroring the whole-body indirect calorimetry data (Fig. 2G). Oxidative phosphorylation capacity with complex I linked substrate revealed an impaired respiration in SOL in the non-stimulated state in TRα^{HSACre} mice relative to WT mice. Assessment of complex I and complex I+II linked respiration identified that T3 stimulation in TRα^{HSACre} raised respiration to an extent similar to that of WT mice. No differences in mitochondrial respiration were observed in the EDL (Fig. 2H).

The mechanisms by which thyroid hormones increase body temperature are elusive. To test a possible role for muscle TRα$_1$ in T3-mediated elevation of body temperature, we measured core body temperature in WT and TRα^{HSACre} mice treated daily with either T3 or vehicle for 7 days. In agreement with previous studies, T3 treatment significantly elevated body temperature in WT mice at both ambient room temperature (22 °C) and

under thermoneutral conditions (30 °C). Notably, TRα^{HSACre} mice treated with T3 responded similarly to WT mice treated with T3 in terms of body temperature increase at both 22 °C and 30 °C (Fig. 2I-J). Together, these findings underscore that 1) thyroid hormone signaling in skeletal muscle does not contribute to T3-induced pyrexia, and 2) thyroid thermogenesis and T3-induced pyrexia are not entirely interconnected processes.

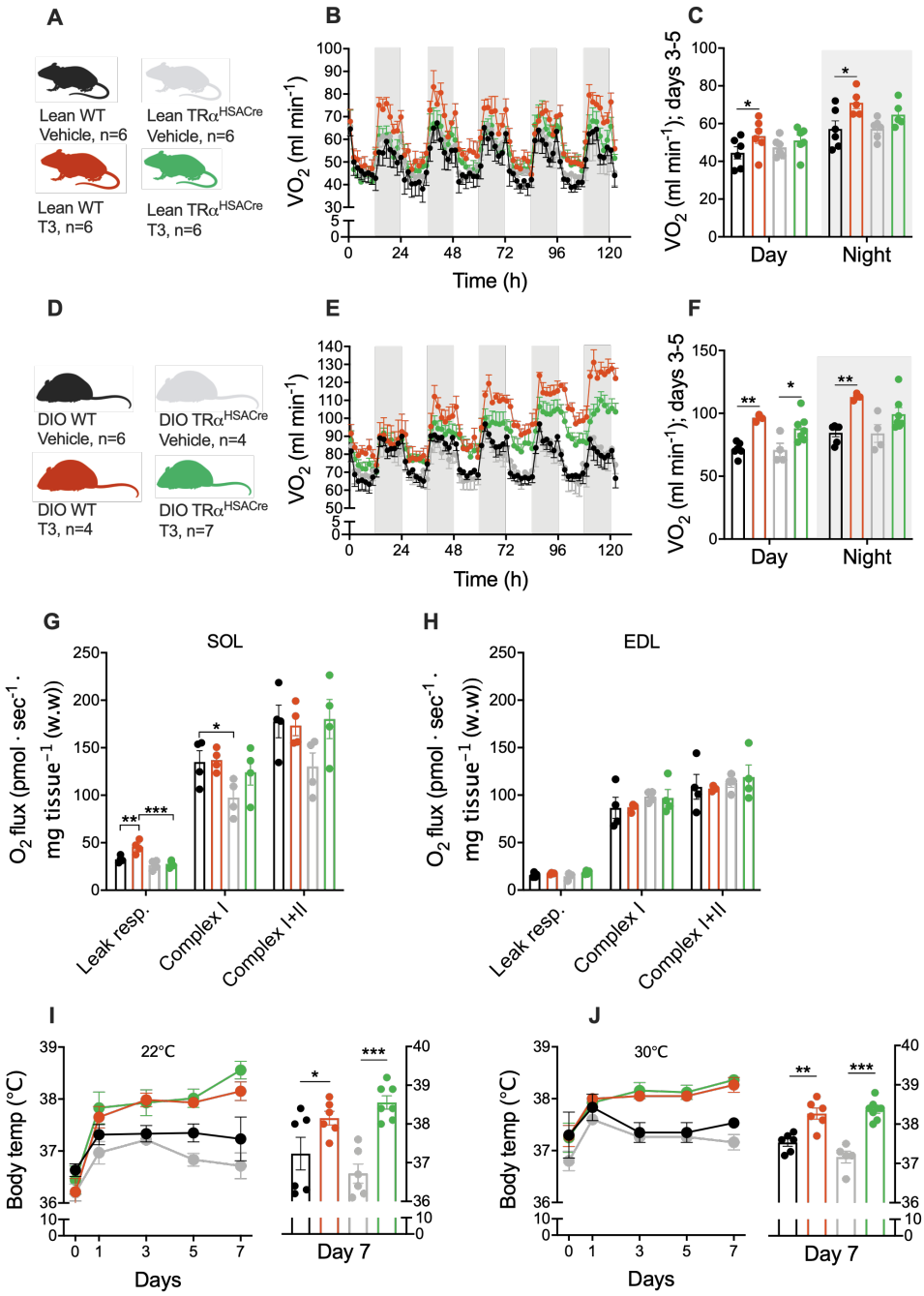

Figure 2. TRα$_1$ in skeletal muscle is essential for T3-mediated increase in energy expenditure but is dispensable for T3-induced pyrexia. **A**, Chow-fed lean WT and TRα^{HSACre} mice were injected daily (s.c.) with either vehicle (WT/ TRα^{HSACre}, n=6/6) or T3 (100 nmol kg^{-1}) (WT/ TRα^{HSACre}, n=6/6) for 5 days. **B**, Effects on longitudinal energy expenditure and (**C**) energy expenditure quantified for days 3-5. **D**, DIO WT and TRα^{HSACre} mice were daily injected (s.c.) with either vehicle (WT/ TRα^{HSACre}, n=6/4) or T3 (WT/ TRα^{HSACre}, n=4/7) for 5 days. **E**, Effects on longitudinal energy expenditure and (**F**) energy expenditure quantified for days 3-5. Chow-fed lean mice WT and TRα^{HSACre} mice were daily injected (s.c.) with either vehicle (WT/ TRα^{HSACre}, n=4/4) or T3 (WT/ TRα^{HSACre}, n=4/4) for 5 days. *Ex vivo* mitochondrial respiration in (**G**) SOL and (**H**) EDL muscles. DIO WT and TRα^{HSACre} mice were daily injected (s.c.) with either vehicle (WT/ TRα^{HSACre}, n=6/6) or T3 (WT/ TRα^{HSACre}, n=6/7) for 7 days. body temperature at (**I**) room temperature and at (**J**) thermoneutral conditions. A one-way ANOVA with selected pairs (treatment vs. genotype) in **G** and **H** or a two-way ANOVA with a Bonferroni post hoc test in **C**, **F**, **I,** and **J** was applied to evaluate differences in genotype and/or treatment. Post hoc analyses were performed irrespective of ANOVA results. *p<0.05, **p<0.01, ***p<0.001. All data are presented as mean ± SEM.

Structural and metabolic pathways dominate the transcriptome in response to T3-mediated activation of TRα$_1$ in soleus muscle

To dissect the mechanistic underpinnings of the muscle-linked induction in whole-body energy expenditure in response to T3 treatment, we performed RNA sequencing (RNA-seq) of WT and TRα^{HSACre} SOL from both treated and non-treated conditions. These analyses revealed that 788 transcripts were differentially expressed between WT SOL and TRα^{HSACre} SOL (Fig. 3A). Under non-stimulated conditions, multiple genes linked to fiber-type composition and muscle morphology were differentially expressed in the TRα^{HSACre} mice compared with WT mice (Fig. 3A). Further, genes associated with muscle thermogenesis, such as sarcolipin and MSS51, were different between genotypes. In response to T3 treatment, expression profiling identified an enrichment of genes with the ontology terms “NADP biosynthesis” and “branched chain amino acids (BCAA) metabolism” to be differentially regulated in T3-treated WT mice but not in T3-treated TRα^{HSACre} mice (Fig. 3B). Relative expression of top T3-responsive transcripts in SOL from WT mice in comparison to TRα^{HSACre} mice revealed a clear distinction in the transcriptional regulation (Fig. 3C). Notably, there is still a clear transcriptional response in SOL to systemic T3 administration despite the mutation of TRα$_1$ in muscle (Fig. 3C). This might reflect systemic effects of T3 that subsequently introduce secondary effects on the muscle transcriptome. Assessment of key genes involved in muscle thermogenesis (Fig. 3D) and muscle fiber-type morphology (Fig. 3E) demonstrated differential expression between WT mice and TRα^{HSACre} mice in both non-stimulated and T3-induced conditions. Notably, the non-stimulated increase in sarcolipin mRNA in the TRα^{HSACre} mice was also present in EDL, gastrocnemius, and quadriceps muscles (Fig. S1F). Markers associated with BAT thermogenesis and thyroid hormone signaling in BAT were examined to determine the specificity of the TRα$_1$-related muscle transcriptional changes (Fig. 3E). Whereas T3 clearly impacts transcripts involved in BAT thermogenesis, no differential expression between TRα^{HSACre} mice relative to WT

mice was observed, implying that the muscle-specific mutation has no systemic "spill-over" to metabolic programs in other thermogenic tissues (Fig. 3F).

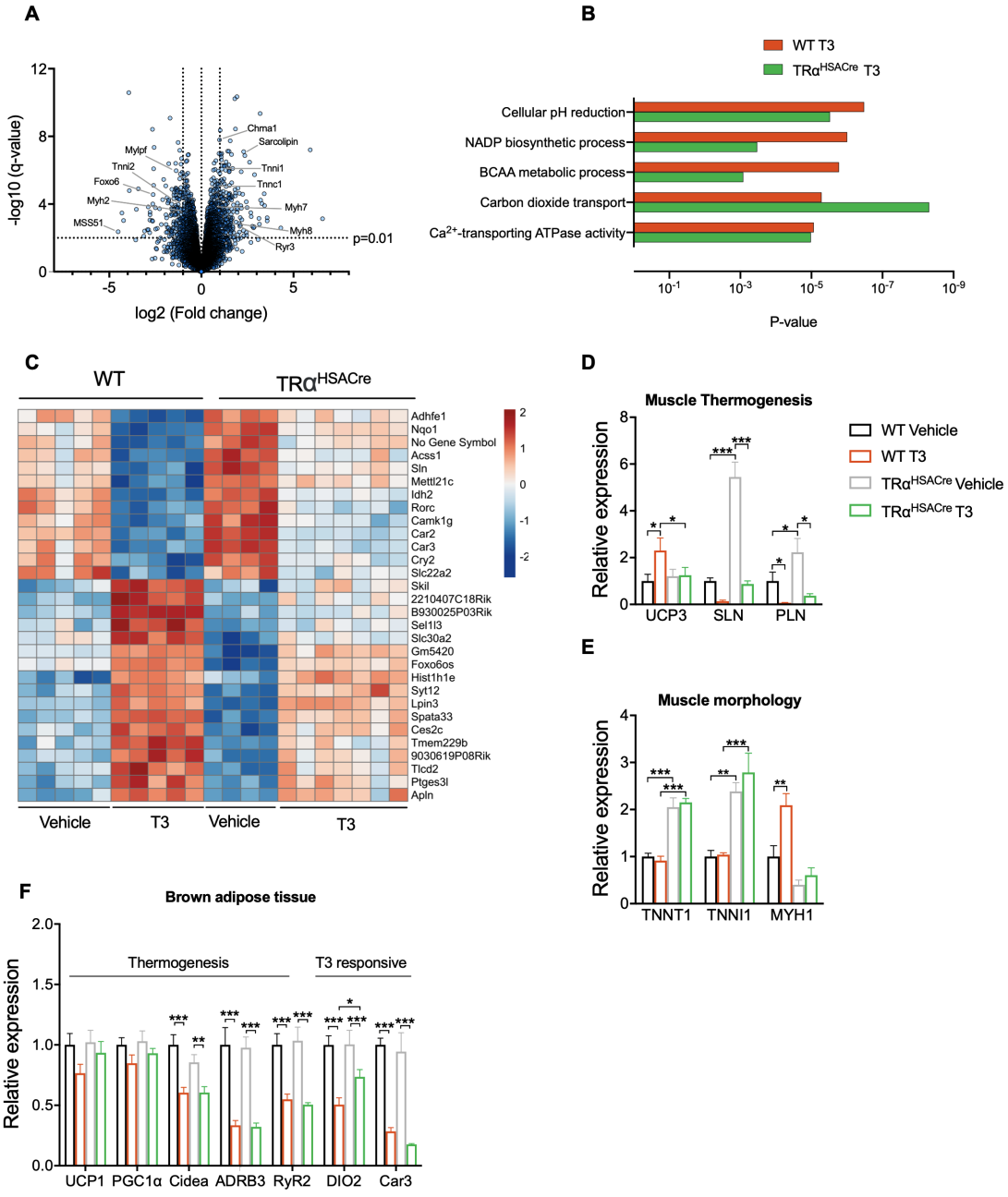

Figure 3. Transcriptome of T3-stimulated TRα$_1$ in soleus muscle

Volcano plot comparing the FDR-adjusted p-values (q-values) and fold change of the TRα^{HSACre} SOL transcriptome relative to WT SOL transcriptome under non-stimulated conditions. **A**, mice were injected daily (s.c.) with vehicle (WT/ TRα^{HSACre}, n=5-6/4-6) or T3 (WT/ TRα^{HSACre}, n=5-6/7) for 7 days. **B**, selected enriched Gene Ontologies that were significantly enriched in T3 treated soleus from WT mice compared to T3 treated SOL from TRα^{HSACre} mice. **C**, Heatmap showing top regulated transcripts in WT T3-treated SOL and TRα^{HSACre} T3-treated SOL. Confirmatory qPCR analyses of transcripts involved in (**D**) muscle thermogenesis, (**E**) muscle morphology, and (**F**) BAT thermogenesis and thyroid hormone action. A one-way ANOVA with selected pairs (treatment vs. genotype)

with a Bonferroni post hoc test was applied to evaluate differences in genotype and/or treatment. Post hoc analyses were performed irrespective of ANOVA results. *p<0.05, **p<0.01, ***p<0.001. All data are presented as mean ± SEM.

DISCUSSION

The coordinated biological mechanisms by which thyroid hormones regulate energy metabolism have been studied for more than 100 years. Yet, the key regulatory pathways remain elusive. Here we use a skeletal muscle-specific TRα_1 loss-of-function mouse model to show that T3-mediated increase in whole-body energy expenditure, in part, relies on thyroid-induced actions in skeletal muscle. Further, we demonstrate that muscle-independent mechanisms govern the increase in body temperature following T3 treatment. Our data support a model by which thyroid hormone actions in muscle promote metabolic rate via coordinated regulation of fiber-type composition, substrate metabolism, and muscle thermogenesis.

It is well established that levels of thyroid hormones impact muscle fiber type characteristics and mitochondrial activity (Argov et al., 1988; Bloise et al., 2018). Thyroid hormone excess induces a shift towards fast-twitch muscle fiber type (Simonides and van Hardeveld, 2008), whereas hypothyroidism leads to slow-twitch muscle phenotype (Caiozzo et al., 2000). The effects of thyroid hormone on muscle is considered to be mediated almost exclusively by TRα_1 (Miyabara et al., 2005; Salvatore et al., 2014). This is supported by global thyroid hormone receptor KO studies showing that deletion of TRα_1 leads to a lower abundance of fast-twitch fibers in SOL and that ablation of TRβ has no consequences on muscle morphology (Yu et al., 2000). Here we expand this knowledge by showing that muscle TRα_1 is necessary for maintaining normal fiber type distribution. Although loss-of-function of TRα_1 in muscle dramatically impacts fiber type composition in slow-twitch muscle, this morphological change has no functional consequence on exercise capacity or voluntary running.

To our surprise, metabolic rate was unperturbed in the TRα^{HSACre} mice under non-stimulated conditions at ambient temperature, and the ability of the TRα^{HSACre} mice to defend body temperature against mild cold stress was also intact. In comparison, global TRα KO mice are reported to be cold intolerant and protected from diet-induced obesity (Pelletier et al., 2008). Important to note, TRα is widely expressed throughout the body, and global TRα KO mice suffer from a series of abnormalities (Flamant and Samarut, 2003). The data presented here suggest that TRα_1 in skeletal muscle is dispensable for body temperature protection against mild cold stress. Conversely, muscle TRα_1 seems to play a minor role in the progression of diet-induced obesity. Here, we employed transcriptomics to identify molecular signals in muscle that could underlie the preserved metabolic rate in the TRα^{HSACre} mice. Notably, sarcolipin expression was increased >5-fold in the TRα^{HSACre} mice in the non-stimulated state. Sarcolipin affects muscle thermogenesis via uncoupling of SERCA-mediated ATP hydrolysis (Smith et al., 2002). Parallel ablation of sarcolipin and BAT thermogenic capacity renders mice cold intolerant, and reintroduction of sarcolipin expression in skeletal muscle rescues the phenotype (Bal

et al., 2012; Rowland et al., 2015). Corroborating an interdependence between BAT and muscle for non-shivering thermogenesis, UCP1 KO mice increase muscle sarcolipin levels in the cold (Bal et al., 2017). Thus, the pronounced increase in sarcolipin expression in $TR\alpha^{HSACre}$ skeletal muscle might represent a compensatory mechanism in the context of impaired thyroid signaling in muscle (Maurya et al., 2015) and suggests a hitherto unrecognized interdependence or crosstalk between thyroid and sarcolipin-mediated signaling and control of muscle thermogenesis.

The most striking observation in the present study is that pharmacological thyroid thermogenesis is largely dependent on muscle $TR\alpha_1$ signaling. This is perhaps surprising given the increased focus on thyroid hormones and BAT thermogenesis over the last decade, but it aligns with recent studies showing that thyroid thermogenesis is intact in UCP1 KO mice (Dittner et al., 2019; Johann et al., 2019). Here, we demonstrate that the T3-mediated elevation in whole-body energy expenditure can be ascribed in part to actions in muscle. Because the indirect calorimetry studies of the present study were executed at ambient temperature (22 °C), a partially retained thermogenic capacity of the BAT might contribute to the quantity of muscle-independent thermogenesis observed in the T3-treated $TR\alpha^{HSACre}$ mice. Further, futile substrate cycling in other tissues, e.g. liver, likely contributes to the increase in whole-body energy expenditure in response to exogenous T3 (Finan et al., 2016).

Another key finding of the present work is that the T3-mediated increase in energy expenditure is partially dissociated from T3-induced defense of an elevated body temperature. Accordingly, we show that $TR\alpha_1$ signaling muscle is not required for T3-induced pyrexia, suggesting that thyroid hormone-mediated increase in body temperature is governed by other organs. A segregation of energy expenditure and body temperature in response to tissue-specific thyroid hormone signaling has been observed previously. A pharmacological study reported that a glucagon-T3 hybrid molecule signals in hepatocytes and adipocytes to increase energy expenditure, without affecting body temperature (Finan et al., 2016). Future studies are warranted to untangle the molecular interconnectedness between energy expenditure and body temperature. In experimental mice, assessment of heat dissipation of the tail surface, in response to pharmacological T3, should be considered in such studies (Warner et al., 2013).

In conclusion, we demonstrate that muscle is a key site for thyroid thermogenesis. Further, we reveal that $TR\alpha_1$ in skeletal muscle is dispensable for T3-governed induction in body temperature, and therefore that thyroid thermogenesis is partially disconnected from T3-induced pyrexia. Our data also show that $TR\alpha_1$ is fundamental for muscle fiber-type composition and, in the absence of $TR\alpha_1$ signaling, molecular compensatory mechanisms appear to safeguard metabolic rate. As such, the present study supports a repositioning of skeletal muscle as a crucial target organ for thyroid hormones in energy metabolism.

MATERIALS AND METHODS

Animals

The thyroid receptor alpha 1 ($TR\alpha_1$) dominant negative mutation L400R was generated as previously described (Quignodon et al., 2007). To selectively express the mutated receptor in skeletal muscle, the HSA-Cre mouse line was used, and $TR\alpha^{flox/flox}$ mice were crossed with WT^{HSACre} mice resulting in $TR\alpha^{+/flox}$ mice with HSA-Cre (referred to as $TR\alpha^{HSACre}$) or Cre negative littermates, which were used as controls (referred to as WT). In Fig. 1J-M, a mixture of Cre negative and WT littermate-mice were used as controls (WT).

Male mice were maintained on a 12 h dark-light cycle housed at 22°C or 30°C. Mice had free access to water and chow diet (Altromin 1324, Brogaarden, DK) or HFD containing 60E% fat (D12492; Research Diets). To study muscle morphology, mice were sacrificed by cervical dislocation, and SOL and EDL muscles were excised and snap frozen in liquid nitrogen. Animal studies were approved by and conducted in accordance with the Danish Animal Experiments Inspectorate.

In vivo pharmacology and energy metabolism studies

Triiodothronine (T3) (Sigma-Aldrich) was administered subcutaneously (s.c.) at 100 nmol per kg body weight (5 µl per gram body weight) in agreement with previous work exploring whole-body energy expenditure in response to T3 (Finan et al., 2016). Body composition was measured by magnetic resonance imaging (EchoMRI-4in1Tm, Echo Medical system LLC, USA). To determine energy expenditure, oxygen (O_2) consumption was measured by indirect calorimetry (TSE System, Germany). O_2 and carbon dioxide (CO_2) were measured every 10 min for five days. Mice were habituated to individual cages three days prior to measurement. For cold challenge, HFD-fed mice were assessed 22 weeks into the dietary intervention, acclimatized to thermoneutral housing before being exposed to an acute 6-hour moderate-cold challenge study, during which the mice were housed at 14 °C. Body temperature was measured using a rectal probe (BIO-TK8851, Bioseblab, France).

Glucose tolerance studies

For assessment of glucose tolerance, mice were fasted for 6 hours, following an intraperitoneal challenge with either 1.75 g (HFD-fed mice) or 2 g (chow-fed mice) glucose per kg body weight. Glucose levels were measured in the blood sampled from the tail veins before (0 min) and at 15, 30, 60, and 120 min post injection using a handheld glucometer (Contour XT, Bayer, CH)

Exercise studies

Voluntary running

Mice were acclimated to running wheels (23 cm in diameter, Techniplast, I) for one week after which running distance and time was measured for 6 weeks, by a computer (Sigma Pure 1 Topline 2016, D) using a magnet affixed to the wheels.

Treadmill running

The week prior the experimental test, mice were acclimated to the treadmill (Treadmill TSE Systems, D) three times at 10 min at 0.17 m s^{-1} at 0° incline. Mice were then exposed to an endurance running test starting with 10 min at 10 m·min^{-1} then 40 min at 27 m·min^{-1} (50% of max speed) with a slope at 10° followed by gradually increased speed (2 m·min^{-1}) until exhaustion. Exhaustion was defined when mice fell back to the grid three times within 30 s. All tests were blinded in terms of genotype.

Transcriptomic analysis by RNA sequencing

Total RNA was isolated using RNeasy mini kit (Qiagen) according to the manufacturers protocol. Messenger RNA sequencing libraries were prepared using the Illumina TruSeq Stranded mRNA protocol (Illumina). Poly-A containing mRNAs were purified by poly-T attached magnetic beads, fragmented, and cDNA was synthesized using SuperScript III Reverse Transcriptase (Thermo Fisher Scientific). cDNA was adenylated to prime for adapter ligation and after a clean-up using AMPure beads (Beckman coulter), the DNA fragments were amplified using PCR followed by a final clean-up. Libraries were quality-controlled using a Bioanalyzer instrument (Agilent Technologies) and subjected to 51-bp paired-end sequencing on a NovaSeq 6000 (Illumina). A total of 1.07 billion reads were generated.

Bioinformatic analysis

The STAR aligner (Dobin et al., 2013) v. 2.7.3a was used to align RNA-seq read against the mm10 mouse genome assembly and GENCODE vM22 mouse transcripts (Frankish et al., 2019). The software program featureCounts v. 1.6.4 was used to summarize reads onto genes (Liao et al., 2014). Testing for differential expression was performed using edgeR[4] v. 3.26.8 using the quasi-likelihood framework with a fitted model of the form *~ 0 + group* where *group* encoded both genotype and treatment (Robinson et al., 2010). Contrasts were constructed as described in the edgeR manual. Gene Ontology[5] enrichments were found using the CAMERA function[7] which is part of the edgeR package (The Gene Ontology, 2019; Wu and Smyth, 2012) . Only gene ontologies with between 5 and 500 genes were investigated.

Quantitative real-time PCR

RNA extraction & cDNA synthesis

Tissues were quickly dissected and frozen either on dry ice or with liquid nitrogen and stored at -80C. Tissue was homogenized in a Trizol reagent (QIAzol Lysis Reagent, Qiagen) using a stainless steel bead (Qiagen)

and a TissueLyser LT (Qiagen) for 3 min at 20 Hz. Then, 200 µl chloroform (Sigma-Aldrich) was added and tubes shaken vigorously for 15 seconds and left at RT for 2 min, followed by centrifugation at 4 °C for 15 min at 12,000 x g. The aqueous phase was mixed 1:1 with 70% ethanol and further processed using RNeasy Lipid Tissue Mini Kit (Qiagen) following the instructions provided by the manufacturer. For muscle tissue, the lysis procedure described in the enclosed protocol in the Fibrous Tissue Mini Kit (Qiagen) was followed. After RNA extraction, RNA content was measured using a NanoDrop 2000 (Thermo Fisher) and 500 ng of RNA was converted into cDNA by mixing FS buffer and DTT (Thermo Fisher) with Random Primers (Sigma-Aldrich) and incubated for 3 min at 70 °C followed by addition of dNTPs, RNase out, Superscript III (Thermo Fisher) and placed in a thermal cycler for 5 min at 25 °C, 60 min at 50 °C, 15 min at 70 °C, and kept at -20 °C until further processing.

qPCR

SYBR green qPCR was performed using Precision plus qPCR Mastermix containing SYBR green or selected probes (Primer Design, #PrecisionPLUS). For primer sequences, see Supplementary Table S1. qPCR was performed in 384-well plates on a Light Cycler 480 Real-Time PCR machine using 2 min preincubation at 95 °C followed by 45 cycles of 60 s at 60 °C, and melting curves were performed by stepwise increasing the temperature from 60 °C to 95 °C. Quantification of mRNA expression was performed according to the delta-delta Ct method.

Mitochondrial respiratory capacity

To study mitochondrial respiration in skeletal muscle, T3-treated and vehicle-treated mice were sacrificed by cervical dislocation. Muscles with different energy metabolism, SOL (oxidative) and EDL (glycolytic), were excised and stored in ice cold relaxing buffer (BIOPS: K_2EGTA (100 mM), Na_2ATP (5.77 mM), $MgCl_2 \cdot 6H_2O$ (6.56 mM), taurine (20 mM), Na_2Phospho-creatine (15 mM), imidazole (20 mM), dithiothreitol (0.5 mM), MES (50 mM), pH = 7.1) and immediately analyzed for mitochondrial respiratory capacity. Mitochondrial respiratory capacity was measured in permeabilized skeletal muscle fibers using high-resolution respirometry (Oroboros Instruments, Innsbruck, Austria). The procedure has been described in detail elsewhere (Boushel et al., 2007). In brief, muscle fibers were dissected in ice cold relaxing buffer (BIOPS) to a high level of fiber separation. Fibers were then placed in ice cold BIOPS containing saponin (50 µg/ml) for 30 min to allow permeabilization of the outer cellular membrane (Kuznetsov et al., 2008). The fibers where then washed twice for 10 min in MiR05 (sucrose (110 mM), potassium lactobionate (60 mM), EGTA (0.5 mM), $MgCl_2$ (3 mM), taurine (20 mM), KH_2PO_4 (10 mM), HEPES (20 mM), BSA (1 g/l), pH 7.1) on ice. Approximately 2 mg was weighed and placed in each Oxygraph chamber. All measurements were carried out in MiR05 at 37 °C after hyperoxygenation to avoid potential oxygen limitation. The following protocol was used in soleus and EDL: malate (2 mM), glutamate (10 mM), and pyruvate (5 mM) were added to determine

state 2 respiration with complex I linked substrates (LEAK). ADP (5 mM) was added to evaluate state 3 respiration with complex I linked substrates (CI_P). Cytochrome *c* (10 µM) was added to control for outer mitochondrial membrane integrity. Finally, succinate (10 mM) was added to evaluate complex I+II linked respiration ($CI+II_P$).

Muscle morphology

SOL and EDL muscles were isolated and snap-frozen on dry ice and embedded in TissueTek and cut in 10 µm transverse sections on a cryostat. The sections were fixed using a mixture of acetone/100% alcohol (1:1) for 20 min. The sections were then pre-incubated in 5% normal donkey serum to block non-specific binding. The mixture of primary antibodies (Developmental Studies Hybridoma Bank, University of Iowa): BA-D5 (IgG2b) specific for MyHC-I, SC-71 (IgG1) specific for MyHC-2A and BF-F3 (IgM) specific for MyHC-2B, was applied to detect the different myosin heavy chain isoforms. Type 2X fibers are not recognized by these antibodies and remain black. For immunofluorescence, the mixture of three different secondary antibodies (Jackson ImmunoResearch): goat anti-mouse IgG1, conjugated with DyLight488 fluorophore (for SC-71); goat anti-mouse IgG2b, conjugated with DyLight405 fluorophore (for BA-D5); goat anti-mouse IgM, conjugated with DyLight549 fluorophore (for BF-F3) was used. After 1-hr incubation with secondary antibodies, sections were washed and embedded with Dako mounting media. Pictures were collected with an epifluorescence Olympus BX61microscope equipped with an Olympus DP71 camera. The relative number composition (%) of each muscle fiber type was analyzed using ImageJ software (NIH).

Blood plasma analyses

Plasma levels of total T3 (DNOV053, NovaTec Immundiagnostica GmbH, Germany), total T4 (EIA-4568 DRG Diagnostics, Germany), and GDF15 (ELISA, R&D systems, catalog no. MGD150) were determined according to instructions provided by the manufacturer.

Statistics

Statistical differences were performed on data distributed in a normal pattern using one- or two-way ANOVA followed by Bonferroni's post hoc analysis as appropriate, or an unpaired two-tailed Student's t-test. Post hoc analyses were performed irrespective of the two-way ANOVA results. All results are presented as mean ± SEM, and $P < 0.05$ was considered significant. Selection of differentially expressed genes and gene ontology enrichments were done based on false discovery adjusted P-values. Analyses were performed using Prism version 8 (GraphPad, US)

Data availability

The raw sequencing data and aligned read counts generated as part of this study has been deposited to the NCBI Sequence Read Archive. Accession number:
GSE146336; https://www.ncbi.nlm.nih.gov/geo/query/acc.cgi?acc=GSE146336. The scripts used for the analysis of the sequencing data and figure generation is available at https://github.com/lars-work-sund/GSE146336.

Acknowledgements

A. M. L. and A. M. F. were supported by a research grant from the Danish Diabetes Academy, which is funded by the Novo Nordisk Foundation, grant number NNF17SA0031406. Furthermore, A. M. F. was supported by the Alfred Benzon Foundation. CC is supported by research grants from the Lundbeck Foundation (Fellowship R238-2016-2859) and the Novo Nordisk Foundation (grant number NNF17OC0026114). Novo Nordisk Foundation Center for Basic Metabolic Research is an independent Research Center, based at the University of Copenhagen, Denmark, and partially funded by an unconditional donation from the Novo Nordisk Foundation (www.cbmr.ku.dk) (Grant number NNF18CC0034900).

Conflict of interest

The other authors have declared that no competing interests exist.

References

Argov, Z., Renshaw, P.F., Boden, B., Winokur, A., and Bank, W.J. (1988). Effects of thyroid hormones on skeletal muscle bioenergetics. In vivo phosphorus-31 magnetic resonance spectroscopy study of humans and rats. J Clin Invest *81*, 1695-1701.

Bal, N.C., Maurya, S.K., Sopariwala, D.H., Sahoo, S.K., Gupta, S.C., Shaikh, S.A., Pant, M., Rowland, L.A., Bombardier, E., Goonasekera, S.A.*, et al.* (2012). Sarcolipin is a newly identified regulator of muscle-based thermogenesis in mammals. Nat Med *18*, 1575-1579.

Bal, N.C., Singh, S., Reis, F.C.G., Maurya, S.K., Pani, S., Rowland, L.A., and Periasamy, M. (2017). Both brown adipose tissue and skeletal muscle thermogenesis processes are activated during mild to severe cold adaptation in mice. J Biol Chem *292*, 16616-16625.

Bloise, F.F., Cordeiro, A., and Ortiga-Carvalho, T.M. (2018). Role of thyroid hormone in skeletal muscle physiology. J Endocrinol *236*, R57-R68.

Boushel, R., Gnaiger, E., Schjerling, P., Skovbro, M., Kraunsoe, R., and Dela, F. (2007). Patients with type 2 diabetes have normal mitochondrial function in skeletal muscle. Diabetologia *50*, 790-796.

Caiozzo, V.J., Haddad, F., Baker, M., McCue, S., and Baldwin, K.M. (2000). MHC polymorphism in rodent plantaris muscle: effects of mechanical overload and hypothyroidism. Am J Physiol Cell Physiol *278*, C709-717.

Dittner, C., Lindsund, E., Cannon, B., and Nedergaard, J. (2019). At thermoneutrality, acute thyroxine-induced thermogenesis and pyrexia are independent of UCP1. Mol Metab *25*, 20-34.

Dobin, A., Davis, C.A., Schlesinger, F., Drenkow, J., Zaleski, C., Jha, S., Batut, P., Chaisson, M., and Gingeras, T.R. (2013). STAR: ultrafast universal RNA-seq aligner. Bioinformatics *29*, 15-21.

Finan, B., Clemmensen, C., Zhu, Z., Stemmer, K., Gauthier, K., Muller, L., De Angelis, M., Moreth, K., Neff, F., Perez-Tilve, D.*, et al.* (2016). Chemical Hybridization of Glucagon and Thyroid Hormone Optimizes Therapeutic Impact for Metabolic Disease. Cell *167*, 843-857 e814.

Flamant, F., and Samarut, J. (2003). Thyroid hormone receptors: lessons from knockout and knock-in mutant mice. Trends Endocrinol Metab *14*, 85-90.

Frankish, A., Diekhans, M., Ferreira, A.M., Johnson, R., Jungreis, I., Loveland, J., Mudge, J.M., Sisu, C., Wright, J., Armstrong, J.*, et al.* (2019). GENCODE reference annotation for the human and mouse genomes. Nucleic Acids Res *47*, D766-D773.

Johann, K., Cremer, A.L., Fischer, A.W., Heine, M., Pensado, E.R., Resch, J., Nock, S., Virtue, S., Harder, L., Oelkrug, R.*, et al.* (2019). Thyroid-Hormone-Induced Browning of White Adipose Tissue Does Not Contribute to Thermogenesis and Glucose Consumption. Cell Rep *27*, 3385-3400 e3383.

Kuznetsov, A.V., Veksler, V., Gellerich, F.N., Saks, V., Margreiter, R., and Kunz, W.S. (2008). Analysis of mitochondrial function in situ in permeabilized muscle fibers, tissues and cells. Nat Protoc *3*, 965-976.

Liao, Y., Smyth, G.K., and Shi, W. (2014). featureCounts: an efficient general purpose program for assigning sequence reads to genomic features. Bioinformatics *30*, 923-930.

Lopez, M., Varela, L., Vazquez, M.J., Rodriguez-Cuenca, S., Gonzalez, C.R., Velagapudi, V.R., Morgan, D.A., Schoenmakers, E., Agassandian, K., Lage, R.*, et al.* (2010). Hypothalamic AMPK and fatty acid metabolism mediate thyroid regulation of energy balance. Nat Med *16*, 1001-1008.

Maurya, S.K., Bal, N.C., Sopariwala, D.H., Pant, M., Rowland, L.A., Shaikh, S.A., and Periasamy, M. (2015). Sarcolipin Is a Key Determinant of the Basal Metabolic Rate, and Its Overexpression Enhances Energy Expenditure and Resistance against Diet-induced Obesity. J Biol Chem *290*, 10840-10849.

Miyabara, E.H., Aoki, M.S., Soares, A.G., Saltao, R.M., Vilicev, C.M., Passarelli, M., Scanlan, T.S., Gouveia, C.H., and Moriscot, A.S. (2005). Thyroid hormone receptor-beta-selective agonist GC-24 spares skeletal muscle type I to II fiber shift. Cell Tissue Res *321*, 233-241.

Mullur, R., Liu, Y.Y., and Brent, G.A. (2014). Thyroid hormone regulation of metabolism. Physiol Rev *94*, 355-382.

Pelletier, P., Gauthier, K., Sideleva, O., Samarut, J., and Silva, J.E. (2008). Mice lacking the thyroid hormone receptor-alpha gene spend more energy in thermogenesis, burn more fat, and are less sensitive to high-fat diet-induced obesity. Endocrinology *149*, 6471-6486.

Quignodon, L., Vincent, S., Winter, H., Samarut, J., and Flamant, F. (2007). A point mutation in the activation function 2 domain of thyroid hormone receptor alpha1 expressed after CRE-mediated recombination partially recapitulates hypothyroidism. Mol Endocrinol *21*, 2350-2360.

Robinson, M.D., McCarthy, D.J., and Smyth, G.K. (2010). edgeR: a Bioconductor package for differential expression analysis of digital gene expression data. Bioinformatics *26*, 139-140.

Rowland, L.A., Bal, N.C., Kozak, L.P., and Periasamy, M. (2015). Uncoupling Protein 1 and Sarcolipin Are Required to Maintain Optimal Thermogenesis, and Loss of Both Systems Compromises Survival of Mice under Cold Stress. J Biol Chem *290*, 12282-12289.

Salvatore, D., Simonides, W.S., Dentice, M., Zavacki, A.M., and Larsen, P.R. (2014). Thyroid hormones and skeletal muscle--new insights and potential implications. Nat Rev Endocrinol *10*, 206-214.

Silva, J.E. (2006). Thermogenic mechanisms and their hormonal regulation. Physiol Rev *86*, 435-464.

Silva, J.E., and Larsen, P.R. (1983). Adrenergic activation of triiodothyronine production in brown adipose tissue. Nature *305*, 712-713.

Silva, J.E., and Larsen, P.R. (1985). Potential of brown adipose tissue type II thyroxine 5'-deiodinase as a local and systemic source of triiodothyronine in rats. J Clin Invest *76*, 2296-2305.

Simonides, W.S., and van Hardeveld, C. (2008). Thyroid hormone as a determinant of metabolic and contractile phenotype of skeletal muscle. Thyroid *18*, 205-216.

Smith, W.S., Broadbridge, R., East, J.M., and Lee, A.G. (2002). Sarcolipin uncouples hydrolysis of ATP from accumulation of Ca2+ by the Ca2+-ATPase of skeletal-muscle sarcoplasmic reticulum. Biochem J *361*, 277-286.

The Gene Ontology, C. (2019). The Gene Ontology Resource: 20 years and still GOing strong. Nucleic Acids Res *47*, D330-D338.

Warner, A., Rahman, A., Solsjo, P., Gottschling, K., Davis, B., Vennstrom, B., Arner, A., and Mittag, J. (2013). Inappropriate heat dissipation ignites brown fat thermogenesis in mice with a mutant thyroid hormone receptor alpha1. Proc Natl Acad Sci U S A *110*, 16241-16246.

Wu, D., and Smyth, G.K. (2012). Camera: a competitive gene set test accounting for inter-gene correlation. Nucleic Acids Res *40*, e133.

Yu, F., Gothe, S., Wikstrom, L., Forrest, D., Vennstrom, B., and Larsson, L. (2000). Effects of thyroid hormone receptor gene disruption on myosin isoform expression in mouse skeletal muscles. Am J Physiol Regul Integr Comp Physiol *278*, R1545-1554.